

Quantitative angiography methods for bifurcation lesions: a consensus statement update from the European Bifurcation Club



Carlos Collet¹, MD; Yoshinobu Onuma², MD, PhD; Rafael Cavalcante³, MD, PhD; Maik Grundeken¹, MD, PhD; Philippe Généreux^{4,5,6,7}, MD; Jeffrey Popma⁸, MD; Ricardo Costa⁹, MD, PhD; Goran Stankovic¹⁰, MD; Shengxian Tu¹¹, MD, PhD; Johan H.C. Reiber¹², PhD; Jean-Paul Aben¹³, PhD; Jens Flensted Lassen¹⁴, MD, PhD; Yves Louvard¹⁵, MD; Alexandra Lansky¹⁶, MD; Patrick W. Serruys^{17*}, MD, PhD

This document is endorsed by the EAPCI.

EAPCI Scientific Documents Committee: Robert A. Byrne¹⁸, MB, BCh, PhD; Davide Capodanno¹⁹, MD

EAPCI review co-ordinator: Ron Waksman²⁰, MD

Document reviewers: Hector-M. Garcia-Garcia²⁰, MD, PhD; Armin Arbab-Zadeh²¹, MD

1. Academic Medical Center, University of Amsterdam, Amsterdam, the Netherlands; 2. Cardialysis BV, Rotterdam, the Netherlands; 3. Erasmus Medical Center, Rotterdam, the Netherlands; 4. Cardiovascular Research Foundation, New York, NY, USA; 5. Columbia University Medical Center, New York, NY, USA; 6. Hôpital du Sacré-Coeur de Montréal, Université de Montréal, Montréal, Québec, Canada; 7. Morristown Medical Center, Morristown, NJ, USA; 8. Beth Israel Deaconess Medical Center, Boston, MA, USA; 9. Dante Pazzanese Institute of Cardiology, Sao Paulo, Brazil; 10. Institute of Cardiovascular Disease, Clinical Center of Serbia, Belgrade, Serbia; 11. Med-X Research Institute, School of Biomedical Engineering, Shanghai Jiao Tong University, Shanghai, China; 12. Medis medical imaging systems bv, Leiden, the Netherlands; 13. Pie Medical Imaging, Maastricht, the Netherlands; 14. Department of Cardiology, The Heart Centre, Rigshospitalet, University of Copenhagen, Copenhagen, Denmark; 15. Institut Hospitalier Jacques Cartier, Massy, France; 16. Yale University, New Haven, CT, USA; 17. Imperial College of London, London, United Kingdom; 18. Deutsches Herzzentrum München, Technische Universität München, Munich, Germany; 19. Ferrarotto Hospital, University of Catania, Catania, Italy; 20. MedStar Cardiovascular Research Network, MedStar Washington Hospital Center, Washington, DC, USA; 21. Department of Medicine/Cardiology Division, Johns Hopkins University, Baltimore, MD, USA

The references are published online at: http://www.pcronline.com/eurointervention/116th_issue/14

KEYWORDS

- bifurcation
- other imaging modalities
- quantitative coronary angiography (QCA)

Abstract

Bifurcation lesions represent one of the most challenging lesion subsets in interventional cardiology. The European Bifurcation Club (EBC) is an academic consortium whose goal has been to assess and recommend the appropriate strategies to manage bifurcation lesions. The quantitative coronary angiography (QCA) methods for the evaluation of bifurcation lesions have been subject to extensive research. Single-vessel QCA has been shown to be inaccurate for the assessment of bifurcation lesion dimensions. For this reason, dedicated bifurcation software has been developed and validated. These software packages apply the principles of fractal geometry to address the “step-down” in the bifurcation and to estimate vessel diameter accurately. This consensus update provides recommendations on the QCA analysis and reporting of bifurcation lesions based on the most recent scientific evidence from *in vitro* and *in vivo* studies and delineates future advances in the field of QCA dedicated bifurcation analysis.

*Corresponding author: Cardiovascular Science Division of the NHLI within Imperial College of Science, Technology and Medicine, South Kensington Campus, London, SW7 2AZ, United Kingdom. E-mail: patrick.w.j.c.serruys@gmail.com

Introduction

The European Bifurcation Club (EBC) is an academic consortium created in 2004 whose goal has been to assess and recommend the appropriate strategies to manage bifurcation lesions¹. In 2009, the EBC assigned to the angiographic subcommittee the task of developing a consensus regarding the appropriate use of quantitative coronary angiography (QCA) for the evaluation of bifurcation lesions. In the previous consensus document, the limitations of single “straight” vessel QCA were addressed with the recommendation for the use of dedicated bifurcation software in clinical practice as well as in clinical trials². Since then there has been increasing evidence of the inaccuracy of single-vessel QCA³. New software for dedicated bifurcation analysis including three-dimensional bifurcation QCA has been developed and validated⁴. Therefore, the aim of this document is to provide an update on the recommendations based on the most recent scientific evidence from *in vitro* and *in vivo* studies and to delineate future advances in the field of QCA dedicated bifurcation analysis.

CORONARY BIFURCATION ANATOMY

Coronary artery branching patterns follow the natural fractal phenomenon⁵. The scaling laws of coronary bifurcation fractal geometry (i.e., the principle of self-similarity at different scales) have been proposed as a guiding tool for percutaneous coronary interventions, to prescribe boundary conditions in fluid dynamic simulations (i.e., shear stress and fractional flow reserve) and, recently, for the development of dedicated bifurcation QCA software⁶⁻⁹.

The relationship among the proximal main vessel (PMV), distal main vessel (DMV) and side branch (SB) has been described by different authors^{7,10}. Finet et al proposed a fractal-like rule $D_{mv} = 0.678 * (D_{dv} + D_{sv})$ to approximate the therapeutic target diameter of the diseased vessels involved in a bifurcation⁷. Subsequently, based on the flow-diameter scaling laws and the conservation of the mass, Huo and Kassab refined the model to $D_{mv}^{7/3} = D_{dv}^{7/3} + D_{sv}^{7/3}$, where D_{mv} , D_{dv} and D_{sv} represent the diameters of the PMV, DMV and SB, respectively¹¹.

These scaling laws provide a simple approach to the heterogeneous and complex coronary tree. They represent the basis for the improvements in quantitative bifurcation analysis to optimise the QCA analysis in bifurcation lesions, resulting in an improvement in predicting lesion severity associated with significant fractional flow reserve (FFR)¹². Of note, some studies have suggested differences in the geometric relationships between left main coronary artery bifurcations (LMCA) and more distal bifurcations (i.e., left anterior descending artery [LAD] and diagonal, left circumflex [LCx] and obtuse marginal [OM]). The curvature between the distal branches (DMV and SB) in the LAD and LCx bifurcations are significantly different from those observed in the LMCA. Also, the LMCA bifurcation has the smallest proximal bifurcation angle and the largest distal angle compared to LAD and LCx bifurcations^{13,14}. Therefore, different anatomical considerations should be taken into account in the assessment of LMCA and distal bifurcations.

Since the introduction of coronary angiography, it has been recognised that visual estimation is inaccurate to quantify coronary stenosis severity¹⁵. This seems to be particularly true for stenosis located at the ostium of the SB in bifurcation lesions, where differences in reference vessel diameters among the three different arterial segments make diameter stenosis assessment more complex¹⁶. In a survey among experts investigating the accuracy of visual assessment compared to quantitative angiography in bifurcations lesions, visual estimation consistently overestimated lesion severity in the DMV and SB. Consequentially, the inter-observer agreement for the visual Medina classification was low, with a significant misclassification of bifurcation lesions compared to a quantitative Medina classification¹⁶. In the quantitative Medina classification, diameter stenosis $\geq 50\%$ is assessed with dedicated bifurcation software in all three segments separately and documented in the same manner as visual Medina classification (e.g., 1,1,1; 1,0,1; 0,0,1; etc.)¹⁷. This issue underscores the need for dedicated quantitative angiographic software to evaluate the extension and severity of disease in a bifurcation lesion.

A fundamental challenge in assessing bifurcations using quantitative angiography methods lies in acquiring the image of the entire bifurcation lesion without significant foreshortening or vessel overlap. While current QCA standards recommend acquiring a minimum of three projections, optimal visualisation of the bifurcation lesion (parent vessel and SB) is typically obtained in one single view. Important morphologic considerations in the assessment of bifurcation lesions, as for all single lesions, have been previously described and include lesion length, ostial side branch location, the extent of calcification, presence of coronary ectasia and irregularity, and markers of plaque instability such as thrombus, plaque ulceration, and flow disturbances. These parameters have been shown to have prognostic significance in procedural and long-term outcomes¹⁸. All of these characteristics should be evaluated and reported individually for the parent vessel and the SB.

LIMITATIONS OF SINGLE-VESSEL QCA IN BIFURCATION LESIONS

Single-vessel QCA software is inaccurate when applied to bifurcation lesions due to the specific anatomical characteristics of bifurcations¹⁹. Single-vessel analysis ignores the bifurcation core (or polygon of confluence) and the step-down phenomenon, and extrapolates non-existing vessel contours across the bifurcation, frequently requiring arbitrary manual corrections impairing reproducibility. At times, this method can create “pseudo-stenosis” in which the minimal lumen diameter (MLD) is incorrectly located at the site of the SB ostium in the middle of the bifurcation core, instead of locating it at the true MLD site (**Figure 1**). Another challenge in QCA of bifurcations is to assess an accurate reference vessel diameter (RVD) to calculate the percent diameter stenosis (%DS). If the single-vessel algorithm is applied to a bifurcation lesion, this will lead to an inaccurate RVD due to the fractal differences in diameters proximal and distal to the bifurcation

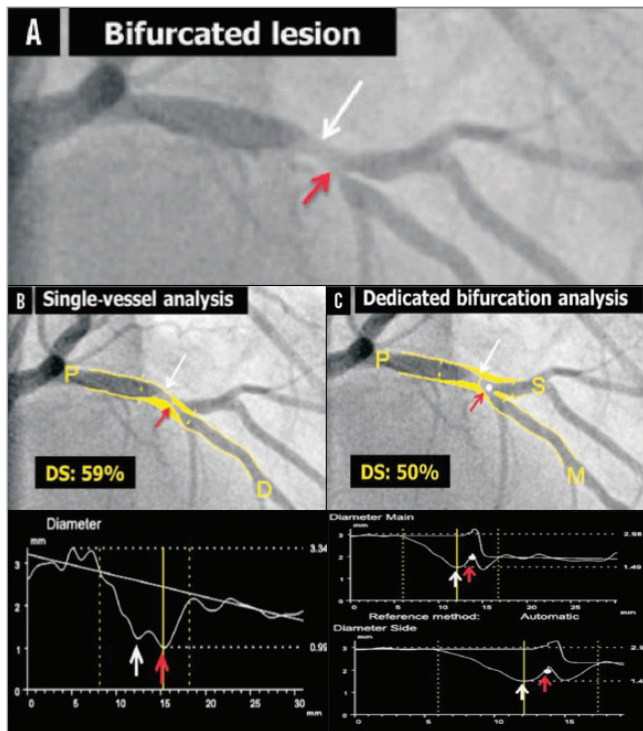


Figure 1. Quantitative coronary angiography of a bifurcation lesion using single-vessel or bifurcation dedicated software. *A*) A bifurcation lesion involving the left anterior descending artery and the first diagonal branch. *B*) Quantitative coronary angiography (QCA) analysis of the bifurcation lesion using single-vessel software creating a “pseudo-stenosis” depicted with a red arrow. *C*) QCA analysis of the same bifurcation lesion using dedicated bifurcation software. In all panels, the white arrow indicates the true location of the MLD of the proximal main branch, the red arrow the pseudo-stenosis found with single-vessel QCA at the actual location of the point of bifurcation (white dot in *C*). MLD: minimum lumen diameter. Reprinted from Grundeken et al²⁰.

(the step-down phenomenon), which is most pronounced at the SB ostium. The interpolated RVD will be overestimated in the ostia of the distal branches because of the larger proximal diameters, thus overestimating the %DS. Conversely, the RVD of the distal part of the PMV will be underestimated, due to the influence of the smaller distal branch on the interpolated RVD²⁰.

Another limitation of the single-vessel approach in bifurcations is the need for manual segment definition, since the software does not recognise where the proximal branch stops and the DMV or SB begins. This factor introduces bias and impairs reproducibility that might undermine trial results²⁰.

DEDICATED BIFURCATION QCA SOFTWARE

To overcome the above-mentioned shortcomings of single-vessel software, dedicated bifurcation QCA algorithms were developed. Three different QCA software packages are currently available. 1. CAAS bifurcation software (Pie Medical Imaging, Maastricht, the Netherlands) (Figure 2).

2. QAngio XA bifurcation software (Medis medical imaging systems, Leiden, the Netherlands) (Figure 3).
3. CardiOp-B System (Paicon Medical Ltd., Rosh Ha'ayin, Israel)^{21,22}.

These systems incorporated principles of fractal geometry to address the “step-down” in the bifurcation and to estimate the reference vessel diameter. The accuracy and precision of the CAAS and QAngio XA bifurcation software packages have been compared *in vitro* with bifurcation plexiglass phantoms and both have proved to be more accurate than single-vessel QCA analysis¹⁹.

COMPARISON OF CONVENTIONAL SINGLE-VESEL ANALYSIS VERSUS DEDICATED BIFURCATION SOFTWARE

To assess the accuracy of the single-vessel software in bifurcation lesions objectively, and to validate both QAngio XA and CAAS bifurcation software algorithms, Ishibashi et al performed a phantom validation study¹⁹. For this analysis, six precision plexiglass phantoms with a total of 18 bifurcations were used. The 18 bifurcations were analysed three times: 1) with the conventional single-vessel algorithm of CAAS (version 5.10), 2) with the bifurcation algorithm of CAAS, and 3) with the bifurcation algorithm of QAngio XA (version 7.3). The single-vessel analysis was performed from the PMV to the DMV and from the PMV to the SB. The study showed that conventional single-vessel analysis underestimated the RVD and %DS in the PMV, while these parameters were overestimated in the DMV and SB (Figure 4). Overall, combining all three segments of the 18 bifurcations (54 segments), the single-vessel approach showed

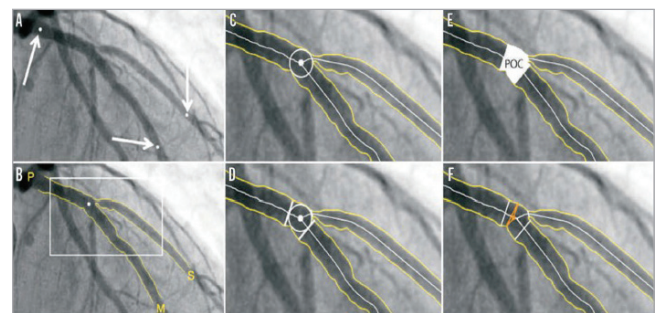


Figure 2. CAAS 2D bifurcation software (Pie Medical Imaging). In the CAAS QCA bifurcation software, the segment of analysis is indicated by one proximal and two distal delimiter points (white arrows, *A*). After automatic detection of the contours (*B*), the “point of bifurcation” (POB) is defined as the mid-point of the largest possible circle touching all three contours (*C*). The intersections of the circle with the centerlines (*D*) indicate the boundaries of the POC (*E*). The diameter values are obtained differently inside the POC from those in straight segments outside the POC (*F*). Outside the POC, diameters are determined by the shortest distance between the vessel’s outer borders, as in the conventional straight-vessel QCA algorithm. Within the POC, however, another mathematical algorithm, the so-called “minimum freedom” approach, is used. Reprinted from Grundeken et al²⁰.

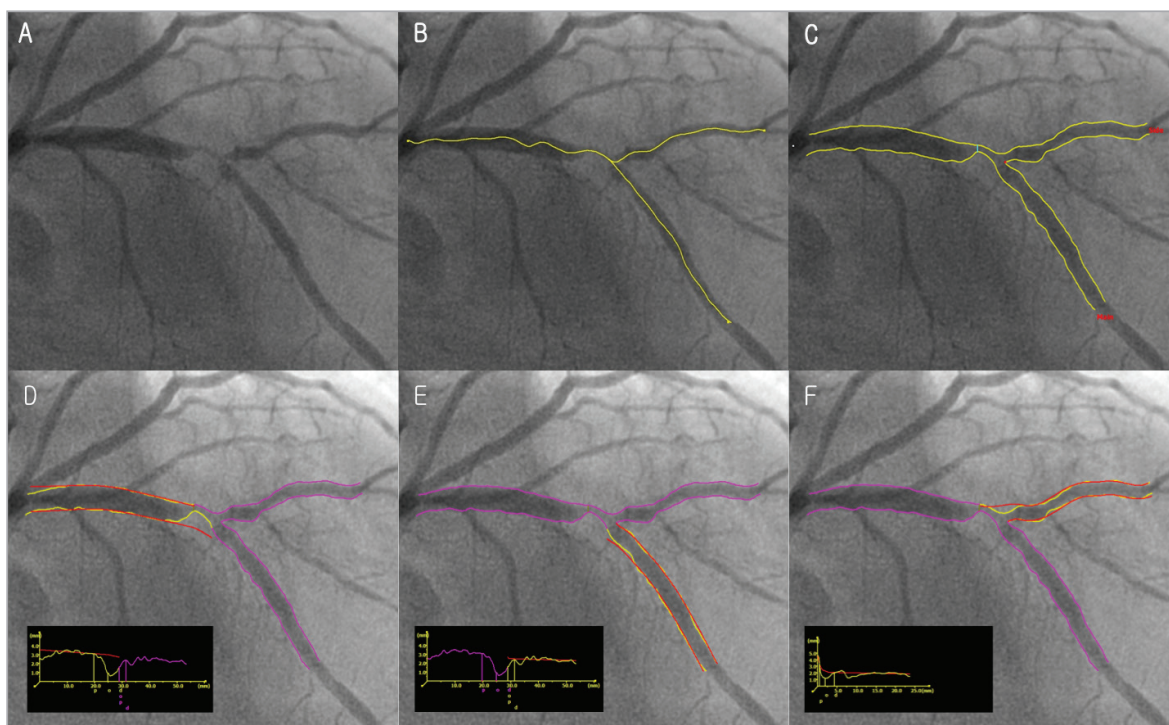


Figure 3. *QAngio XA bifurcation software (Medis). A) A left anterior descending artery-diagonal branch bifurcation lesion. B) First, the analyst defines the segment of analysis by indicating one start point in the proximal vessel and one endpoint in each of the two distal branches, after which two wavepath pathlines from proximal to distal are detected (note that the proximal parts overlap). C) Subsequently, the vessel contours are automatically detected using the minimal cost algorithm (MCA). In addition to the vessel contours, the initial position of the carinal point and the proximal delimiter (independent of the presence of lesions) are automatically detected (red dot and light blue line, respectively), in order to define the vessel bifurcation with a model of four building blocks and its measurements, D and E). The T-shape's arterial and reference diameter functions are determined using the Medis straight vessel diameter function for the proximal and distal main branch sections, subsequently combined in the middle by an interpolated diameter function for the bifurcation core transition. F) An adjusted Medis ostial diameter function is used for the side branch, reconstructing a proximal flare to correspond to the "mouth" of the ostium. Reprinted from Grundeken et al²⁰.*

poor accuracy and precision for RVD and %DS. The bifurcation algorithms, on the other hand, proved to be highly accurate and precise, with comparable accuracy and precision between the CAAS and QAngio XA (with systematic use of the T-shape model) bifurcation software with regard to MLD, RVD, and %DS¹⁹. This study demonstrates that the use of the single-vessel QCA approach is inaccurate in bifurcation lesions. It also validated the CAAS and QAngio XA bifurcation software packages for quantitative angiographic assessment of coronary bifurcations.

The differences between single-vessel analysis and dedicated bifurcation software were also observed in a clinical trial evaluating a dedicated bifurcation coronary stent³. From the population of the randomised trial comparing a Dedicated Bifurcation Stent Versus Provisional Stenting in the Treatment of Coronary Bifurcation Lesions (TRYTON Bifurcation Study), 326 (46%) patients underwent planned repeat angiography at nine months²³. The use of single-vessel QCA analysis was systematically associated with a higher in-stent %DS at the level of the SB (bias 5.54% [CI -26.74 to 37.82]) compared with dedicated two-dimensional (2D) bifurcation analysis³.

THREE-DIMENSIONAL DEDICATED QCA SOFTWARE

To overcome potential limitations associated with 2D quantitative coronary analysis of bifurcation lesions (i.e., vessel overlap, tortuosity and foreshortening), dedicated three-dimensional (3D) quantitative coronary analysis (QCA) software packages have been developed^{4,24,25}.

By combining two 2D image data sets, the new 3D bifurcation software is able to perform a 3D reconstruction of the bifurcation and determine lumen dimensions and bifurcation angle. Furthermore, the best single view can be calculated based on the 3D bifurcation geometry allowing X-ray angiographic optimal visualisation of the bifurcation lesion. In order to reconstruct the bifurcation core into a 3D image correctly, the fact that the contour information obtained from the 2D projections may contain vessel overlap needs to be taken into account, since the bifurcated vessel might be partly obscured in one or both of the image projections.

In the CAAS 7.3 QCA 3D system, the identification of a common image point (CIP) corrects for the distortion introduced by the isocentre offset before the 3D centrelines are reconstructed by means of an adaptive 3D epipolar geometry algorithm²⁴.

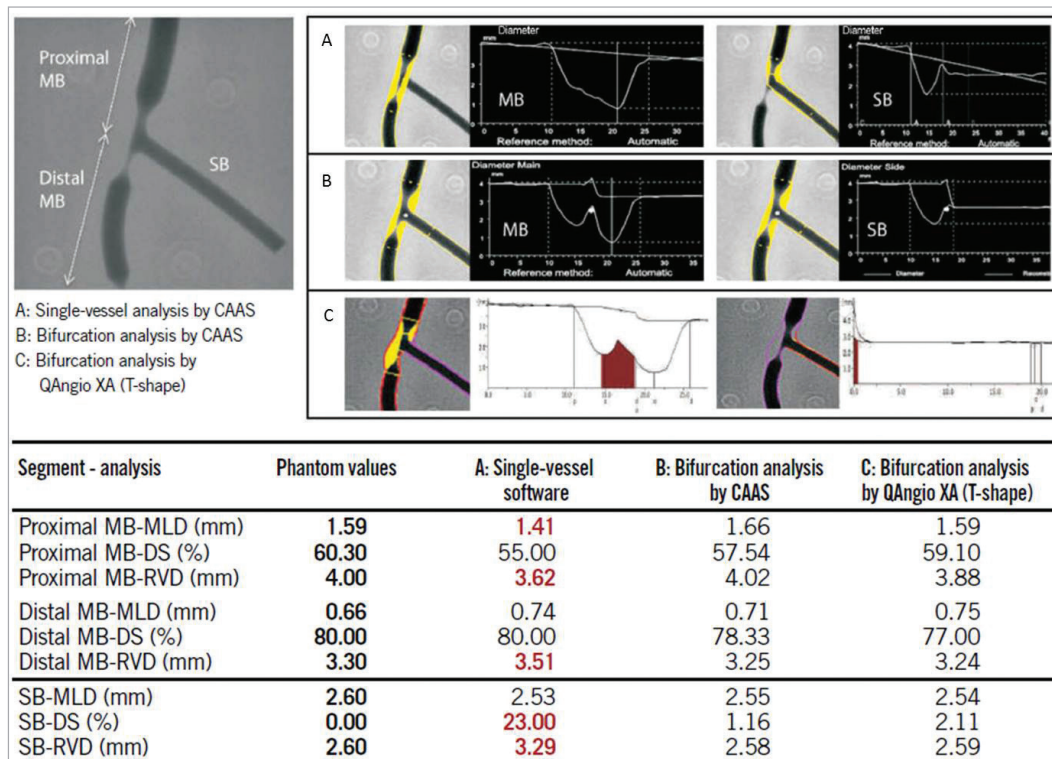


Figure 4. Quantitative coronary angiography measurement by CAAS and QAngio XA software for a bifurcated lesion in the calibrated phantom. Angiographic parameters including reference diameter (RVD), minimal lumen diameter (MLD), % diameter stenosis (%DS) are given in the PMV, DMV, and side branch (SB). A cine-angiogram demonstrated moderate to severe stenosis both in the proximal main vessel (PMV) and in the distal main vessel (DMV) with a Medina class 1,1,0. The conventional single-vessel method measured a significantly smaller RVD in the PMV and a larger RVD in the DMV and SB. A) QCA using the conventional single-vessel algorithm by CAAS. B) QCA using the bifurcation algorithm by CAAS. C) QCA using the T-shape bifurcation algorithm by QAngio XA. QCA: quantitative coronary angiography. Reprinted from Grundeken et al²⁰.

Respective 3D cross-sections are constructed assuming an elliptical model, by using the luminal diameters of the corresponding 2D cross-sections and their spatial orientations to define the ellipse axes. Analogous to previous CAAS bifurcation analysis, the polygon of confluence (POC) is defined as the central bifurcation region which behaves differently from a single-vessel analysis²⁶. Outside the POC, the cross-sectional area is defined perpendicular to the centre of the lumen; within the POC, the cross-sectional area is defined by the smoothest possible surface that spans the lumen at each centreline position resulting in curved cross-sections within the central bifurcation region. Automatic calculation of reference cross-sectional area adopts the methodology described for CAAS 2D bifurcation QCA and applies it to the 3D reconstructed model. Outside the POC, a 3D equivalent of the algorithm used in single-vessel segments is employed^{4,27}. Within the POC, the reference area is derived by applying an interpolation technique between the “healthy” reconstructed 3D branches. Based on the respective cross-sectional areas, lumen diameter and RVD are defined as the equivalent diameters based on the assumption of circularity (Figure 5).

In the QAngio XA 3D (RE) software, an automatic correction for the system distortion is performed by means of one to three pairs

of offset correction points and their corresponding epipolar lines¹⁴. As a first step, the calculation of the reference diameter function is based on each of the three segments separately, with the assumption that there is no tapering in reference diameter within each segment. Subsequently, these three reference diameter functions are used to reconstruct the reference core diameter function, taking into account the distal bifurcation angle. Instead of assessing the diameters along several flat planes at the bifurcation core, this new bifurcation model creates a number of bent oval planes, with the degree of bending depending on the distal bifurcation angle. The bending of the oval planes linearly decreases from the carina position towards the proximal, changing into a flat plane at the beginning of the bifurcation core. The sum of the two paired diameters at each bent oval plane defines the core diameter. Accordingly, the reference core diameter is defined as the sum of the paired reference diameters at each oval plane (Figure 6)^{12,28}. Finally, with both 3D software packages, two bifurcation angles are computed between the PMV and the SB (proximal angle or angle A), and between the DMV and the SB (distal angle or angle B) (Figure 7). Bifurcation angles are calculated in 3D space without overlap, and theoretically are more precise than 2D QCA. Although the feasibility of 3D QCA analysis has been reported to be limited, pre-specified angiographic

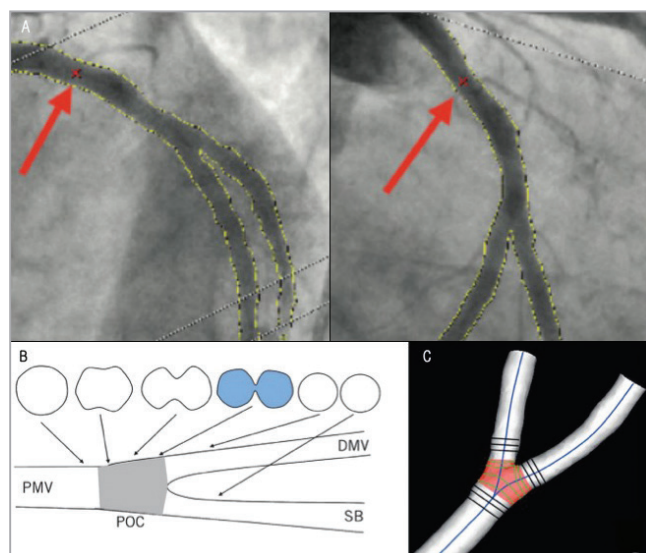


Figure 5. CAAS QCA 3D bifurcation methodology. Automatic selection of common imaging points (CIP, red crosses indicated with red arrows) in two different projections (A). The analysis can optimise the position of CIP manually if necessary. Definition of polygon of confluence (POC). B) Within POC (grey) the vessel is slowly widening, but at the same time the top and bottom are slowly collapsing towards a single point (figure-of-eight shape in blue, panel B) after which we have two “normal”-shaped vessels. C) The start of the POC (in red) is defined as the position where plane cross-sections give way to curved ones; exactly the opposite marks the end of the POC. DMV: distal main vessel; PMV: proximal main vessel; POC: polygon of confluence; SB: side branch. Reprinted from Onuma et al²⁴.

acquisition guidelines and novel algorithms that compensate for the isocentre offset can improve the feasibility of this analysis²⁹.

The accuracy of the CAAS 3D bifurcation software has been evaluated *in vitro* using a bifurcation phantom³⁰. In 3D reconstructions based on two 2D images⁴, acquired at variable rotation and angulation, accuracy and precision (mean difference±SD) of the 11-segment model for MLD, RVD and DS were 0.013 ± 0.131 mm, -0.052 ± 0.039 mm and $-1.08\pm 5.13\%$, respectively; inter-observer variability was 0.141 mm, 0.058 mm and 5.42%, respectively. Accuracy and precision for bifurcation angle (BA) was $-1.3\pm 5.0^\circ$, whereas inter-observer variability was 7.5° ; respective measures for length were 0.15 ± 0.26 mm and 0.54 mm⁴. There was also an *in vivo* validation of the CAAS 3D QCA with intravascular ultrasound as a reference. Coronary luminal areas were shown to be highly correlated with systematic underestimation of lumen area of 0.45 ± 1.49 mm²³¹. During the same period, the accuracy of the QAngio XA 3D (RE) software was evaluated using a silicone bifurcation phantom³². The accuracy and precision for angle assessment was $0.4\pm 1.1^\circ$ for proximal BA and $1.5\pm 1.3^\circ$ for distal BA. The intra- and inter-observer variabilities for the proximal BA were $0.3\pm 1.0^\circ$ and $0.5\pm 0.9^\circ$, and for the distal BA were $0.8\pm 1.0^\circ$ and $0.3\pm 0.8^\circ$. In addition, the QAngio XA 3D (RE)

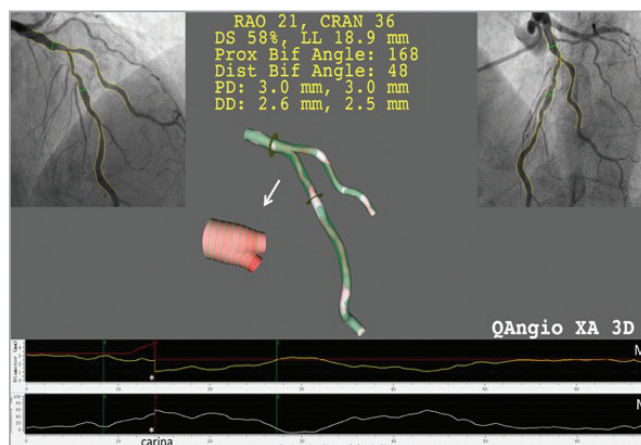


Figure 6. Three-dimensional vessel reconstruction and quantitative analysis of a stenosis at a left anterior descending artery and diagonal bifurcation with QAngio XA 3D (RE). The top left and top right panels show the two angiographic views used for 3D reconstruction. The reconstructed lumen and reference surface of the bifurcation are shown in the middle panel. M) The lumen and reference diameter functions for the left anterior descending artery (LAD) including the bifurcation core. N) The stenosis function for the LAD. Note that the stenosis function jumps at the carina (asterisk) due to the relatively higher stenosis in the LAD than in the diagonal ostium.

software was compared *in vivo* with intravascular ultrasound and optical coherence tomography. A high correlation and a small bias in luminal areas between 3D QCA and IVUS ($r=0.799$, $p<0.001$; bias $+1.21$ mm² [limits of agreement -2.09 to 4.51]) and 3D QCA and OCT ($r=0.897$, $p<0.001$; bias $+1.07$ mm² [limits of agreement -1.85 to 3.99]) were found³³.

A comparison between 2D and 3D dedicated bifurcation software was performed in the setting of a sub-analysis of a randomised trial assessing a dedicated bifurcation device³⁴. Muramatsu et al

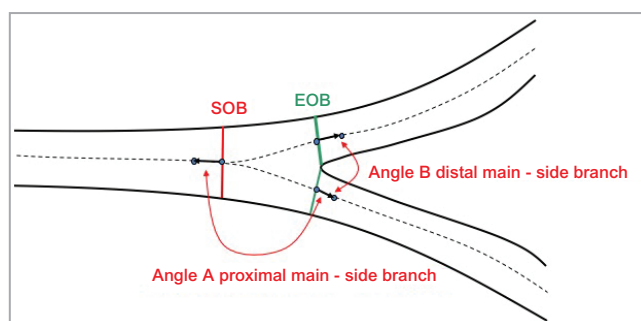


Figure 7. Calculation of bifurcation angles. Two bifurcation angles are computed between the proximal main vessel (PMV) and the SB (proximal angle or angle A), and between the distal main vessel (DMV) and the SB (distal angle or angle B); they are derived from a 3D vector of the centreline in the PMV at the start of the bifurcation core (directed from distal to proximal) and 3D vectors of the centrelines in the DMV and SB at the distal end of the bifurcation core.

analysed pre- and post-procedure angiographies in 114 patients treated with a dedicated side branch bifurcation stent. In the treated segments, there were no differences in MLD between 2D and 3D, while diameter stenosis was significantly higher in 2D compared to 3D analysis both pre-procedure and post procedure (53.9% for 2D vs. 52.1% for 3D pre-procedure, $p < 0.01$; 23.2% for 2D vs. 20.9% for 3D post procedure, $p = 0.01$). In the sub-segment level analysis, lengths of PMV, DMV and SB were consistently shorter in 2D compared to 3D both pre-procedure and post procedure. Notably, using 3D QCA, the anatomic location of the smallest MLD or the highest DS was relocated to a different bifurcation sub-segment in a considerable proportion of the patients compared to when 2D QCA was used (kappa values: 0.50 for MLD, 0.55 for %DS)³⁴. Also, in another study Yong et al showed that 3D QCA-derived measurements showed better predictive ability in detecting functionally significant stenosis determined by invasive FFR as compared to 2D QCA-derived measurements in simple lesions³⁵. Indeed, the use of 3D QCA analysis improved the predictive ability in determining a positive FFR, compared with the straight vessel analysis¹². Therefore, the dedicated bifurcation 3D QCA algorithm may provide more accurate information; nevertheless, more studies comparing 2D and 3D software in bifurcation lesions are needed.

Three-dimensional QCA also enables determination of the optimal viewing angle of a bifurcation lesion, i.e., the angulation and rotation characterised by having an orthogonal view of the bifurcation, minimising vessel foreshortening and overlap³⁶. Tu et al found that the “true” optimal viewing angles could not be obtained since the angles were too deep to be obtained by the X-ray systems, suggesting that measurement of bifurcation angles by 2D QCA is unreliable in a high portion of routine clinical acquisitions due to suboptimal 2D angiographic views. In this study of 194 bifurcations, the proximal BA in LAD/diagonal, LCx/OM, and PDA/PLA were comparable and not statistically different ($p = 0.133$), being $151^\circ \pm 13^\circ$, $146^\circ \pm 18^\circ$, and $145^\circ \pm 19^\circ$, respectively. However, the distal BA in LAD/diagonal were smaller than LCx/OM ($p = 0.004$) and PDA/PLA ($p = 0.001$), being $48^\circ \pm 16^\circ$ vs. $57^\circ \pm 16^\circ$, and $59^\circ \pm 17^\circ$, respectively. The left main bifurcation had the smallest proximal BA ($128^\circ \pm 24^\circ$) and the largest distal BA ($80^\circ \pm 21^\circ$)¹⁴.

In addition, 3D QCA analysis of the bifurcation angle on the left main coronary artery has been shown to impact on prognosis. In a study by Girasis et al, a restricted post-procedural systolic-diastolic distal bifurcation angle range ($< 10^\circ$) resulted in higher five-year adverse event rates after LM bifurcation percutaneous coronary interventions²⁹.

Future perspectives

Functional assessment of coronary stenosis has proved to be essential for the indication of revascularisation procedures as the angiographic anatomic assessment alone might sometimes be insufficient for defining the need for treatment³⁷. Studies with FFR have demonstrated that the correlation of coronary %DS and ischaemia can be especially challenging in bifurcation lesions, particularly at the level of the SB. As shown by Koo et al, a high

discrepancy between angiographic (%DS $\geq 75\%$) and functional criteria (FFR < 0.75) exists for the evaluation of SB lesions³⁸. Sarno et al, using a dedicated 2D bifurcation QCA software, found a moderate correlation ($r = 0.57$, $p = 0.02$) between angiographic (%DS $\geq 50\%$) and functional criteria (FFR < 0.80) for the assessment of lesion severity at the level of the SB³⁹. Also, the 3D QCA dedicated bifurcation software (QAngio XA 3D [RE]) was tested in 78 bifurcation lesions using FFR as the reference. A moderate correlation between invasive FFR and diameter stenosis was found ($\rho = -0.50$, $p < 0.001$)¹².

Recently, a computational approach to derive FFR from coronary X-ray angiography has been developed (Figure 8, Figure 9)⁴⁰⁻⁴². The combination of angio-derived FFR and dedicated bifurcation QCA could further refine the evaluation of bifurcation lesions. These tools combined could be useful for defining treatment necessity, selecting the procedural strategy and assessing success. However, these novel approaches need further validation.

Multislice computed tomography coronary angiography (MSCT) has been increasingly used as a non-invasive alternative to conventional invasive angiography for the assessment of coronary anatomy to guide the treatment decision and help procedure planning (e.g., to define the best angiographic projection for a specific lesion)⁴³. A computational algorithm that calculates the fractional flow reserve non-invasively on the MSCT images (FFR_{CT}) has also been developed and has been introduced into clinical practice with promising results⁴⁴. In addition, this technology has been used to stent coronary lesions “virtually”. This feature could be utilised to plan complex bifurcation interventions based on the FFR_{CT} in the main branch and side branch after virtual stenting. This non-invasive tool might also be useful in the assessment and treatment planning of coronary bifurcation lesions.

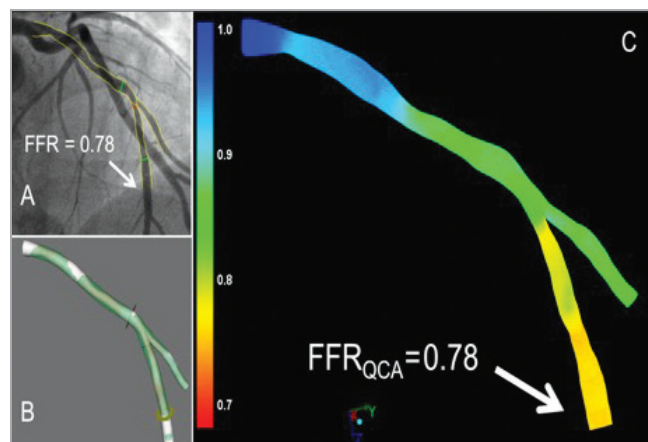


Figure 8. Examples of the FFR derived from angiography using the QAngio XA 3D (RE) (Medis) bifurcation model. The angiogram with the invasive FFR measurement (FFR=0.78) is shown in panel A. Panels B and C show the 3D reconstruction and the angiography-derived FFR (QFR). In this case the FFR and QFR match precisely, both being 0.78 at the distal location of the main branch, as indicated by the arrows. FFR: fractional flow reserve

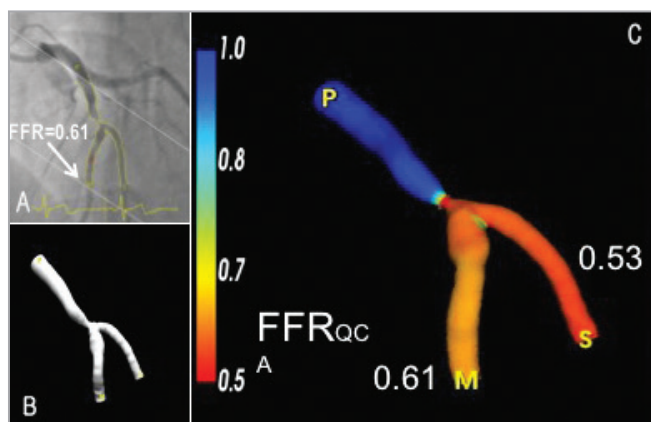


Figure 9. Illustrative examples of the FFR derived from angiography using the CAAS QCA 3D (Pie Medical Imaging). A) One of the two angiographic projections used to generate the 3D reconstruction of the bifurcation LAD and 2nd diagonal as shown in panel B. C) The 3D reconstruction including the angiography-derived FFR. In this example, the angiography-derived FFR at the distal location of the main branch was 0.61 and 0.53 for the side branch. Invasive FFR measurement within the main branch was 0.62. FFR: fractional flow reserve

In the future, the investigation of flow and shear stress derived from angiography with pulsatile non-Newtonian simulations might show the complexities and intricacies of the pathology in coronary bifurcations. A combined anatomical and functional evaluation may supersede a purely angiographic assessment, as seen in the non-bifurcated pathology.

RECOMMENDATIONS FOR QCA ANALYSIS AND REPORTING IN CORONARY BIFURCATION LESIONS

In order to obtain standardised reporting of QCA analyses, the consensus group recommends the following:

1. Three angiographic projections orthogonal to the bifurcation plane should be acquired for optimal visualisation of the lesion. These projections should be separated by at least 30° to facilitate dedicated QCA bifurcation analysis. The quantitative analysis should be performed in two views with no vessel overlap, minimal foreshortening and displaying the widest bifurcation angle².
2. A qualitative assessment of the bifurcation lesion (such as calcification, the presence of thrombus) should be reported in each of the three segments.
3. The 2D or 3D angles between the proximal main vessel and the side branch (proximal BA) and between the distal main vessel and side branch (distal BA) should be reported pre-intervention, post intervention and at follow-up since they are relevant for the selection of the PCI technique and long-term clinical events^{29,45}.
4. In addition to the visual Medina classification, the quantitative Medina classification should be used to assess and to classify the bifurcation lesion severity and define the treatment strategy^{16,46}.

5. Single-vessel analysis of bifurcation lesions should be abandoned². For the quantitative analysis of bifurcation lesions, dedicated 2D or 3D bifurcation software packages should be used to assess lesion dimensions, severity and extension using a segmental analysis. In the segmental analysis, MLD, RVD and %DS should be reported for each coronary segment (PMV, DMV and SB). As a basic report, we recommend using the six-segment model (PMV, DMV, SB, 5 mm proximal segment, 5 mm distal segment in the main vessel and 5 mm distal segment in the SB). Additionally, the segmentation of the ostia of the SB and DMV, the entire main vessel, and the entire side branch could be reported (**Figure 10**).
6. To assess the significance of the SB, the size of the side branch should be defined as the reference vessel diameter at the ostium of the SB (segment 8).
7. The highest percent diameter stenosis (%DS) with the corresponding MLD should be reported as one metric for the entire bifurcation lesion.
8. A segmental analysis using the bifurcation segment model at the time of pre-intervention and post intervention and follow-up should be reported. This segmental analysis should provide a detailed analysis of the location of residual stenosis post intervention and the precise location of treatment failure or restenosis at follow-up².
9. At follow-up, binary restenosis should be reported in each of the three segments separately, resulting in quantitative Medina scores at each follow-up time point to give an idea about bifurcation lesion complexity at baseline, post procedure, and follow-up^{16,46}.

Conclusions

Most challenges in quantitative coronary angiography assessment of bifurcation lesions have been addressed by new software developments that have been validated in *in vitro* and in clinical studies. The introduction of 3D QCA software represents a further step in the field. These new QCA packages allow a precise anatomical bifurcation assessment with the possibility of assessing the functional component of the coronary bifurcation (i.e., angiography-derived FFR). However, validation of this new software for bifurcation lesions is still required to determine the future application of this technology.

Impact on daily practice

The precise evaluation of coronary bifurcation lesions is of paramount importance for defining the need for intervention and to guide treatment strategy. Dedicated bifurcation quantitative coronary angiography (QCA) analysis provides an accurate assessment of the bifurcation geometry and dimensions. In clinical practice, and in the research setting, dedicated QCA packages are the recommended approach for assessing bifurcation lesions pre and post intervention. For consistency in reporting clinical trials in the field of bifurcation lesions, a list of recommendations for QCA analysis is provided in this consensus document.

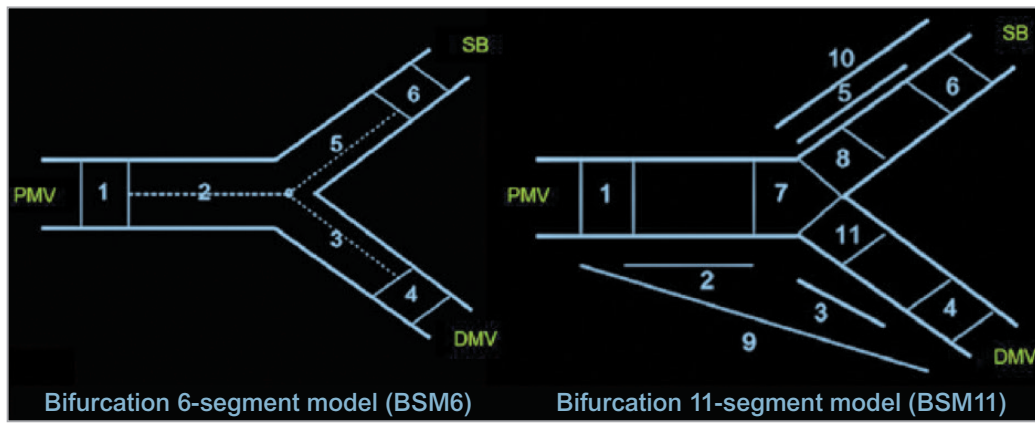


Figure 10. Bifurcation segment models. A composite of segments 2, 3, and 5 in the bifurcation six-segment model (BSM6) corresponds to the “treated segment,” where the stents were implanted or balloons were dilated, including the proximal main vessel (PMV), distal main vessel (DMV) and side branch (SB). The segments 2, 3, and 5 are divided by the point of bifurcation (POB), defined as the point where all the centrelines meet and the mid-point of the largest circle/sphere that can reach all three contours in bifurcation. Segments 1, 4, and 6 correspond to 5 mm segments beyond the treated segment (left panel). Segment 8 in BSM11 reflects 3 mm ostial segments of the SB (right panel). Reprinted from Girasis et al⁴.

Conflict of interest statement

Y. Onuma is a member of the International Advisory Board of Abbott Vascular. P. Généreux received speaker fees from Abbott Vascular, Cardiovascular Systems Inc., Tryton Medical, Edwards Lifesciences and AstraZeneca, and a research grant from Boston Scientific and Cardiovascular Systems Inc., is a consultant for Cardiovascular Systems Inc. and Soundbite Medical Solutions Inc., and is an equity holder of Soundbite Medical Solutions Inc. J. Popma received institutional grants from Medtronic, Abbott Vascular and Boston Scientific and is a member of the Boston Scientific Medical Advisory Board. S. Tu received a research grant from Medis medical imaging systems bv. J.H.C. Reiber is the CEO of Medis medical imaging systems bv. J-P. Aben is the CEO of Pie Medical Imaging. P.W. Serruys is a member of the International Advisory Board of Abbott Vascular. The other authors have no conflicts of

interest to declare. The Guest Editor is a consultant for Abbott Vascular, Biosensors International, Biotronik, Boston Scientific, Medtronic Vascular, Symetis, Lifetech, is on the speakers’ bureau of AstraZeneca, Boston Scientific, Biotronik, and Abbott Vascular, and has received grant support from Biosensors International, Biotronik, Boston Scientific, Edwards Lifesciences, and Abbott Vascular.

References

The references can be found in the online version of this article.

The supplementary data are published online at:
http://www.pcronline.com/eurointervention/116th_issue/14



Supplementary data

References

- Lassen JF, Holm NR, Banning A, Burzotta F, Lefèvre T, Chieffo A, Hildick-Smith D, Louvard Y, Stankovic G. Percutaneous coronary intervention for coronary bifurcation disease: 11th consensus document from the European Bifurcation Club. *EuroIntervention*. 2016;12:38-46.
- Lansky A, Tuinenburg J, Costa M, Maeng M, Koning G, Popma J, Cristea E, Gavit L, Costa R, Rares A, Van Es GA, Lefevre T, Reiber H, Louvard Y, Morice MC; European Bifurcation Angiographic Sub-Committee. Quantitative angiographic methods for bifurcation lesions: a consensus statement from the European Bifurcation Group. *Catheter Cardiovasc Interv*. 2009;73:258-66.
- Grundeken MJ, Ishibashi Y, Génereux P, LaSalle L, Iqbal J, Wykrzykowska JJ, Morel MA, Tijssen JG, de Winter RJ, Girasis C, Garcia-Garcia HM, Onuma Y, Leon MB, Serruys PW. Inter-core lab variability in analyzing quantitative coronary angiography for bifurcation lesions: a post-hoc analysis of a randomized trial. *JACC Cardiovasc Interv*. 2015;8:305-14.
- Girasis C, Schuurbiens JC, Muramatsu T, Aben JP, Onuma Y, Soekhradj S, Morel MA, van Geuns RJ, Wentzel JJ, Serruys PW. Advanced three-dimensional quantitative coronary angiographic assessment of bifurcation lesions: methodology and phantom validation. *EuroIntervention*. 2013;8:1451-60.
- Bassingthwaighte JB, Van Beek JH, King RB. Fractal branchings: the basis of myocardial flow heterogeneities? *Ann N Y Acad Sci*. 1990;591:392-401.
- Finet G, Huo Y, Rioufol G, Ohayon J, Guerin P, Kassab GS. Structure-function relation in the coronary artery tree: from fluid dynamics to arterial bifurcations. *EuroIntervention*. 2010;6 Suppl J:J10-5.
- Finet G, Gilard M, Perrenot B, Rioufol G, Motreff P, Gavit L, Prost R. Fractal geometry of arterial coronary bifurcations: a quantitative coronary angiography and intravascular ultrasound analysis. *EuroIntervention*. 2008;3:490-8.
- Taylor CA, Fonte TA, Min JK. Computational fluid dynamics applied to cardiac computed tomography for noninvasive quantification of fractional flow reserve: scientific basis. *J Am Coll Cardiol*. 2013;61:2233-41.
- van der Giessen AG, Groen HC, Doriot PA, de Feyter PJ, van der Steen AF, van de Vosse FN, Wentzel JJ, Gijzen FJ. The influence of boundary conditions on wall shear stress distribution in patients specific coronary trees. *J Biomech*. 2011;44:1089-95.
- Huo Y, Kassab GS. Scaling laws of coronary circulation in health and disease. *J Biomech*. 2016;49:2531-9.
- Huo Y, Finet G, Lefèvre T, Louvard Y, Moussa I, Kassab GS. Optimal diameter of diseased bifurcation segment: a practical rule for percutaneous coronary intervention. *EuroIntervention*. 2012;7:1310-6.
- Tu S, Echavarría-Pinto M, von Birgelen C, Holm NR, Pyxaras SA, Kumsars I, Lam MK, Valkenburg I, Toth GG, Li Y, Escaned J, Wijns W, Reiber JH. Fractional flow reserve and coronary bifurcation anatomy: a novel quantitative model to assess and report the stenosis severity of bifurcation lesions. *JACC Cardiovasc Interv*. 2015;8:564-74.
- Ellwein L, Marks DS, Migrino RQ, Foley WD, Sherman S, LaDisa JF Jr. Image-based quantification of 3D morphology for bifurcations in the left coronary artery: Application to stent design. *Catheter Cardiovasc Interv*. 2016;87:1244-55.
- Tu S, Jing J, Holm NR, Onsea K, Zhang T, Adriaenssens T, Dubois C, Desmet W, Thuesen L, Chen Y, Reiber JH. In vivo assessment of bifurcation optimal viewing angles and bifurcation angles by three-dimensional (3D) quantitative coronary angiography. *Int J Cardiovasc Imaging*. 2012;28:1617-25.
- Nallamothu BK, Spertus JA, Lansky AJ, Cohen DJ, Jones PG, Kureshi F, Dehmer GJ, Drozda JP Jr, Walsh MN, Brush JE Jr, Koenig GC, Waites TF, Gantt DS, Kichura G, Chazal RA, O'Brien PK, Valentine CM, Rumsfeld JS, Reiber JH, Elmore JG, Krumholz RA, Weaver WD, Krumholz HM. Comparison of clinical interpretation with visual assessment and quantitative coronary angiography in patients undergoing percutaneous coronary intervention in contemporary practice: the Assessing Angiography (A2) project. *Circulation*. 2013;127:1793-800.
- Girasis C, Onuma Y, Schuurbiens JC, Morel MA, van Es GA, van Geuns RJ, Wentzel JJ, Serruys PW; 5th meeting of the European Bifurcation Club. Validity and variability in visual assessment of stenosis severity in phantom bifurcation lesions: a survey in experts during the fifth meeting of the European Bifurcation Club. *Catheter Cardiovasc Interv*. 2012;79:361-8.
- Gil RJ, Bil J, Grundeken MJ, Kern A, Inigo Garcia LA, Vassilev D, Pawlowski T, Formuszewicz R, Dobrzycki S, Wykrzykowska JJ, Serruys PW. Regular drug-eluting stents versus the dedicated coronary bifurcation sirolimus-eluting BiOSS LIM® stent: the randomised, multicentre, open-label, controlled POLBOS II trial. *EuroIntervention*. 2016;12:e1404-e1412.
- Ellis SG, Vandormael MG, Cowley MJ, DiSciascio G, Deligonul U, Topol EJ, Bulle TM. Coronary morphologic and clinical determinants of procedural outcome with angioplasty for multivessel coronary disease. Implications for patient selection. Multivessel Angioplasty Prognosis Study Group. *Circulation*. 1990;82:1193-202.
- Ishibashi Y, Grundeken MJ, Nakatani S, Iqbal J, Morel MA, Génereux P, Girasis C, Wentzel JJ, Garcia-Garcia HM, Onuma Y, Serruys PW. In vitro validation and comparison of different software packages or algorithms for coronary bifurcation analysis using calibrated phantoms: implications for clinical practice and research of bifurcation stenting. *Catheter Cardiovasc Interv*. 2015;85:554-63.
- Grundeken MJ, Ishibashi Y, Ramcharitar S, Tuinenburg JC, Reiber JH, Tu S, Aben JP, Girasis C, Wykrzykowska JJ, Onuma Y,

- Serruys PW. The need for dedicated bifurcation quantitative coronary angiography (QCA) software algorithms to evaluate bifurcation lesions. *EuroIntervention*. 2015;11 Suppl V:V44-9.
21. Gradaus R, Mathies K, Breithardt G, Böcker D. Clinical assessment of a new real time 3D quantitative coronary angiography system: evaluation in stented vessel segments. *Catheter Cardiovasc Interv*. 2006;68:44-9.
 22. Ramcharitar S, Daeman J, Patterson M, van Guens RJ, Boersma E, Serruys PW, van der Giessen WJ. First direct in vivo comparison of two commercially available three-dimensional quantitative coronary angiography systems. *Catheter Cardiovasc Interv*. 2008;71:44-50.
 23. Généreux P, Kumsars I, Lesiak M, Kini A, Fontos G, Slagboom T, Ungi I, Metzger DC, Wykrzykowska JJ, Stella PR, Bartorelli AL, Fearon WF, Lefèvre T, Feldman RL, LaSalle L, Francese DP, Onuma Y, Grundeken MJ, Garcia-Garcia HM, Laak LL, Cutlip DE, Kaplan AV, Serruys PW, Leon MB. A randomized trial of a dedicated bifurcation stent versus provisional stenting in the treatment of coronary bifurcation lesions. *J Am Coll Cardiol*. 2015;65:533-43.
 24. Onuma Y, Girasis C, Aben JP, Sarno G, Piazza N, Lokkerbol C, Morel MA, Serruys PW. A novel dedicated 3-dimensional quantitative coronary analysis methodology for bifurcation lesions. *EuroIntervention*. 2011;7:629-35.
 25. Tu S, Huang Z, Koning G, Cui K, Reiber JH. A novel three-dimensional quantitative coronary angiography system: In-vivo comparison with intravascular ultrasound for assessing arterial segment length. *Catheter Cardiovasc Interv*. 2010;76:291-8.
 26. Ramcharitar S, Onuma Y, Aben JP, Consten C, Weijers B, Morel MA, Serruys PW. A novel dedicated quantitative coronary analysis methodology for bifurcation lesions. *EuroIntervention*. 2008;3:553-7.
 27. Girasis C, Schuurbiens JC, Onuma Y, Aben JP, Weijers B, Morel MA, Wentzel JJ, Serruys PW. Advances in two-dimensional quantitative coronary angiographic assessment of bifurcation lesions: improved small lumen diameter detection and automatic reference vessel diameter derivation. *EuroIntervention*. 2012;7:1326-35.
 28. Tu S, Holm NR, Koning G, Huang Z, Reiber JH. Fusion of 3D QCA and IVUS/OCT. *Int J Cardiovasc Imaging*. 2011;27:197-207.
 29. Girasis C, Farooq V, Diletti R, Muramatsu T, Bourantas CV, Onuma Y, Holmes DR, Feldman TE, Morel MA, van Es GA, Dawkins KD, Morice MC, Serruys PW. Impact of 3-dimensional bifurcation angle on 5-year outcome of patients after percutaneous coronary intervention for left main coronary artery disease: a sub-study of the SYNTAX trial (synergy between percutaneous coronary intervention with taxus and cardiac surgery). *JACC Cardiovasc Interv*. 2013;6:1250-60.
 30. Girasis C, Schuurbiens JC, Onuma Y, Serruys PW, Wentzel JJ. Novel bifurcation phantoms for validation of quantitative coronary angiography algorithms. *Catheter Cardiovasc Interv*. 2011;77:790-7.
 31. Schuurbiens JC, Lopez NG, Ligthart J, Gijssen FJ, Dijkstra J, Serruys PW, Van der Steen AF, Wentzel JJ. In vivo validation of CAAS QCA-3D coronary reconstruction using fusion of angiography and intravascular ultrasound (ANGUS). *Catheter Cardiovasc Interv*. 2009;73:620-6.
 32. Tu S, Holm NR, Koning G, Maeng M, Reiber JH. The impact of acquisition angle differences on three-dimensional quantitative coronary angiography. *Catheter Cardiovasc Interv*. 2011;78:214-22.
 33. Tu S, Xu L, Ligthart J, Xu B, Witberg K, Sun Z, Koning G, Reiber JH, Regar E. In vivo comparison of arterial lumen dimensions assessed by co-registered three-dimensional (3D) quantitative coronary angiography, intravascular ultrasound and optical coherence tomography. *Int J Cardiovasc Imaging*. 2012;28:1315-27.
 34. Muramatsu T, Grundeken MJ, Ishibashi Y, Nakatani S, Girasis C, Campos CM, Morel MA, Jonker H, de Winter RJ, Wykrzykowska JJ, Garcia-Garcia HM, Leon MB, Serruys PW, Onuma Y; TRYTON Pivotal IDE Coronary Bifurcation Trial Investigators. Comparison between two- and three-dimensional quantitative coronary angiography bifurcation analyses for the assessment of bifurcation lesions: A subanalysis of the TRYTON pivotal IDE coronary bifurcation trial. *Catheter Cardiovasc Interv*. 2015;86:E140-9.
 35. Yong AS, Ng AC, Brieger D, Lowe HC, Ng MK, Kritharides L. Three-dimensional and two-dimensional quantitative coronary angiography, and their prediction of reduced fractional flow reserve. *Eur Heart J*. 2011;32:345-53.
 36. Tu S, Hao P, Koning G, Wei X, Song X, Chen A, Reiber JH. In vivo assessment of optimal viewing angles from X-ray coronary angiography. *EuroIntervention*. 2011;7:112-20.
 37. van Nunen LX, Zimmermann FM, Tonino PA, Barbato E, Baumbach A, Engstrom T, Klauss V, MacCarthy PA, Manoharan G, Oldroyd KG, Ver Lee PN, Van't Veer M, Fearon WF, De Bruyne B, Pijls NH; FAME Study Investigators. Fractional flow reserve versus angiography for guidance of PCI in patients with multivessel coronary artery disease (FAME): 5-year follow-up of a randomised controlled trial. *Lancet*. 2015;386:1853-60.
 38. Koo BK, Park KW, Kang HJ, Cho YS, Chung WY, Youn TJ, Chae IH, Choi DJ, Tahk SJ, Oh BH, Park YB, Kim HS. Physiological evaluation of the provisional side-branch intervention strategy for bifurcation lesions using fractional flow reserve. *Eur Heart J*. 2008;29:726-32.
 39. Sarno G, Garg S, Onuma Y, Girasis C, Tonino P, Morel MA, van Es GA, Pijls N, Serruys PW. Bifurcation lesions: Functional assessment by fractional flow reserve vs. anatomical assessment using conventional and dedicated bifurcation quantitative coronary angiogram. *Catheter Cardiovasc Interv*. 2010;76:817-23.
 40. Tu S, Sybren Westra J, Yang J, Li Y, Holm NR, Reiber JH. Functional coronary assessment based on three-dimensional quantitative coronary angiography. In: Escaned J, Serruys PW, eds. *Coronary Stenosis: Imaging, Structure and Physiology*. Toulouse, France: Europa Digital & Publishing; 2015.
 41. Papafaklis MI, Muramatsu T, Ishibashi Y, Lakkas LS, Nakatani S, Bourantas CV, Ligthart J, Onuma Y, Echavarría-Pinto M,

Tsirka G, Kotsia A, Nikas DN, Mogabgab O, van Geuns RJ, Naka KK, Fotiadis DI, Brilakis ES, Garcia-Garcia HM, Escaned J, Zijlstra F, Michalis LK, Serruys PW. Fast virtual functional assessment of intermediate coronary lesions using routine angiographic data and blood flow simulation in humans: comparison with pressure wire - fractional flow reserve. *EuroIntervention*. 2014;10:574-83.

42. Tu S, Barbato E, Koszegi Z, Yang J, Sun Z, Holm NR, Tar B, Li Y, Rusinaru D, Wijns W, Reiber JH. Fractional flow reserve calculation from 3-dimensional quantitative coronary angiography and TIMI frame count: a fast computer model to quantify the functional significance of moderately obstructed coronary arteries. *JACC Cardiovasc Interv*. 2014;7:768-77.

43. Otsuka M, Sugahara S, Umeda K, Nakamura M, Nakamura A, Bonkohara Y, Tsurumi Y. Utility of multislice computed tomography as a strategic tool for complex percutaneous coronary intervention. *Int J Cardiovasc Imaging*. 2008;24:201-10.

44. Norgaard BL, Leipsic J, Gaur S, Seneviratne S, Ko BS, Ito H, Jensen JM, Mauri L, De Bruyne B, Bezerra H, Osawa K, Marwan M, Naber C, Erglis A, Park SJ, Christiansen EH, Kaltoft A, Lassen JF, Botker HE, Achenbach S; NXT Trial Study Group. Diagnostic performance of noninvasive fractional flow reserve derived from coronary computed tomography angiography in suspected coronary artery disease: the NXT trial (Analysis of Coronary Blood Flow Using CT Angiography: Next Steps). *J Am Coll Cardiol*. 2014;63:1145-55.

45. Dzavik V, Kharbanda R, Ivanov J, Ing DJ, Bui S, Mackie K, Ramsamujh R, Barolet A, Schwartz L, Seidelin PH. Predictors of long-term outcome after crush stenting of coronary bifurcation lesions: importance of the bifurcation angle. *Am Heart J*. 2006;152:762-9.

46. Medina A, Suarez de Lezo J, Pan M. [A new classification of coronary bifurcation lesions]. *Rev Esp Cardiol*. 2006;59:183.